JOURNAL OF SOLID STATE CHEMISTRY 28, 379–384 (1979)

Magnetic and Electrical Properties and Mössbauer Effect in the Solid Solution $Fe(Nb_{1-x}W_x)O_4$ $(0 \leq x \leq 1)$

Y. NODA, M. SHIMADA, AND M. KOIZUMI

The Institute of Scientific and Industrial Research, Osaka University, Suita, Osaka 565, Japan

AND F. KANAMARU

Research Institute for Noncrystalline Materials, School of Engineering, Okayama University, Okayama 700, Japan

Received June 2, 1978; in revised form August 31, 1978

The solid solution $Fe(Nb_{1-x}W_x)O_4$ $(0 \leq x \leq 1)$ with wolframite-type structure has been prepared under argon atmosphere at 1000°C. The change of unit cell parameters is not linear, owing to the zigzag chain of octahedra along the c-axis. The results of magnetic susceptibility and Mössbauer effect measurements indicate the existence of a mixed valence state of iron ions.

Introduction

$FeNbO_4$ with wolframite-type structure shows a polymorphic transition, wolframite $\leftrightarrow \alpha$–$PbO_2 \leftrightarrow$ rutile, induced by temperature change (*1*). On the other hand, $FeWO_4$ has only the wolframite-type structure (*2*).

As shown in Fig. 1, the wolframite-type structure has zigzag chains along the c-axis which consist of AO_6 and BO_6 octahedra sharing two edges. According to the results of the magnetic structure for $FeWO_4$ reported by Ülku (*3*), the superexchange magnetic coupling of Fe^{2+}–O–Fe^{2+} along the c-axis is ferromagnetic and that of Fe^{2+}–O–W^{6+}–O–Fe^{2+} is antiferromagnetic. Due to the existence of these two kinds of magnetic coupling, $FeWO_4$ is antiferromagnetic with a Néel temperature of 66°K. On the other hand, the magnetic properties of $FeNbO_4$ have not been investigated so far.

The magnetic and electrical properties of $AMoO_4$, AWO_4 (A = Mn, Fe, Co, Ni), $ATaO_4$ (A = Ti, V, Cr, Fe), and solid solution $(Fe_{1-x}Mn_x)WO_4$ were studied by Van Uitert *et al.* (*4*), Rozhdestvenskii *et al.* (*5*), Astrov *et al.* (*6*), and Obermayer *et al.* (*7*). Crystal chemistry, the changes of site occupation, and the valence states of cations

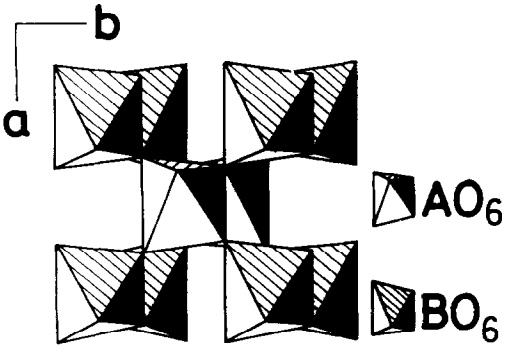

FIG. 1. Crystal structure of wolframite.

0022-4596/79/060379-06$02.00/0

accompanied by the polymorphic transition were studied using the Mössbauer effect parameters for $FeMoO_4$ (*8*) and $FeVO_4$ (*9*).

Mixed valency compounds, in which transition metal ions at identical lattice sites have different valence states, show interesting properties such as high electrical conductivity and double magnetic exchange interaction resulting from exchange of $3d$ electrons. One of the typical examples is the metal–nonmetal transition observed for Fe_3O_4 (*10*).

Since the valence states of cations for $FeNbO_4$ and $FeWO_4$ are deduced to be Fe^{3+} and Nb^{5+} for the former and Fe^{2+} and W^{6+} for the latter, it is expected that in a solid solution of the $Fe^{3+}Nb^{5+}O_4$–$Fe^{2+}W^{6+}O_4$ system, iron ions at octahedral sites will be in mixed valence states, if Nb^{5+} and W^{6+} ions keep their own valence states.

In the present study, an attempt was made to synthesize the complete series of solid solutions of $Fe(Nb_{1-x}W_x)O_4$ and the behavior of $3d$ electrons in these compounds was investigated.

Experimental

The polycrystalline powder compounds in the system of $Fe(Nb_{1-x}W_x)O_4$ $(0 \leqq x \leqq 1)$ were prepared by firing the mixture of Fe_2O_3, Nb_2O_5, and WO_3 powders in a stream of argon at 1000°C for 24 hr and quenching in air to room temperature.

Unit cell parameters were determined from X-ray powder diffraction patterns using silicon as an internal standard.

Magnetic susceptibilities were measured by the conventional Faraday method from room temperature to liquid nitrogen temperature.

Mössbauer absorption spectra were measured using a 400-channel analyzer at room and liquid nitrogen temperatures. The γ-ray source, ^{57}Co in Pd metal, was kept at room temperature. The velocity scale was calibrated by using iron metal as a standard absorber.

The electrical resistivity of the sintered sample was measured using a four-probe technique in the temperature range 150 to 300°K.

Results and Discussion

(*1*) *Lattice Parameters*

The complete series of solid solutions of $Fe(Nb_{1-x}W_x)O_4$ was synthesized, and their X-ray powder patterns were indexed on the basis of wolframite-type structure with orthorhombic symmetry. Figure 2 shows lattice parameters as a function of mole fraction x. It is found that the lattice parameters of the a- and b-axes increase almost linearly, and the c-axis decreases nonlinearly with increasing x. Although the relation of lattice parameters vs mole fraction x did not obey Vegard's law, the fact that the unit cell volume increased linearly with increasing x indicated that the distance between zigzag chains composed of octahedrons sharing two edges was linearly elongated, but the chain itself shrank along the c-axis.

When Nb^{5+} ions are replaced by W^{6+} ions in the $Fe(Nb_{1-x}W_x)O_4$ system, the valence state of iron ions located at octahedral site changes from Fe^{3+} to Fe^{2+}. Since the ionic radius of Fe^{3+} (0.645 Å) is smaller than that

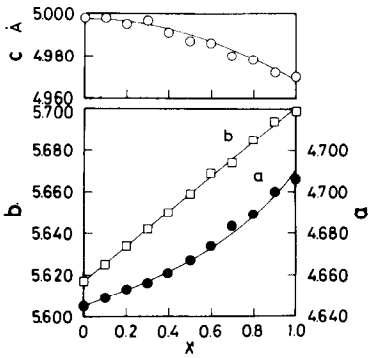

FIG. 2. Lattice parameters vs mole fraction for $Fe(Nb_{1-x}W_x)O_4$.

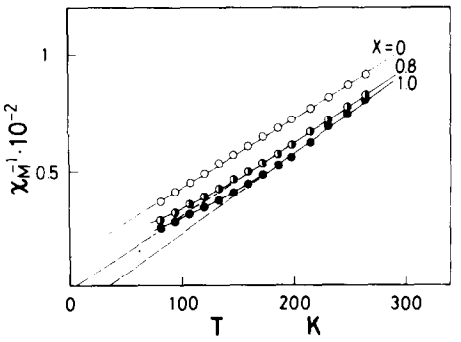

FIG. 3. Reciprocal magnetic susceptibility vs temperature for $Fe(Nb_{1-x}W_x)O_4$.

of Fe^{2+} (0.770 Å) and the radius of Nb^{5+} (0.64 Å) is larger than that of W^{6+} (0.58 Å), shrinkage of the (Nb, W)O_6 octahedron and expansion of the (Fe^{3+}, Fe^{2+})O_6 octahedron occur simultaneously due to the replacement of Nb by W ions. Consequently, the complex changes in dimension along the zigzag chain in the wolframite structure are observed as discussed above.

(2) Magnetic Properties

The temperature dependences of the reciprocal magnetic susceptibilities of $Fe(Nb_{1-x}W_x)O_4$ ($x = 0$, 0.8, 1.0) are shown in Fig. 3. The χ^{-1} vs T curves obey the Curie–Weiss law at higher temperatures.

In Fig. 4, the effective magnetic moments per formula unit are shown as a function of the mole fraction. The value of 4.85 μ_B for $FeWO_4$ ($x = 1.0$) is well interpreted by assuming that the Fe^{2+} ion is in its high-spin state ($S = 2$) (W^{6+} has no magnetic moment). On the other hand, the value of 5.12 μ_B for $FeNbO_4$ ($x = 0$) does not agree with the value calculated by assuming that Fe^{3+} is in its high-spin state ($S = \frac{5}{2}$) (Nb^{5+} has no magnetic moment). In Fig. 4, the broken line represents the calculated μ_{eff} values as a function of x, assuming that Fe^{3+} and Fe^{2+} are in their high-spin states in $(Fe^{3+}_{1-x}Fe^{2+}_x)(Nb^{5+}_{1-x}W^{6+}_x)O_4$. As seen in this figure, observed values lie on the calculated line in the range $0.3 \leqq x \leqq 1.0$, while in the range $0 \leqq x < 0.3$ the observed values deviate from the calculated values. The values of the paramagnetic Curie temperature Θ are negative for the composition of $0 \leqq x \leqq 0.6$, but in the range $0.7 \leqq x \leqq 1.0$ they are positive. This indicates that the dominant magnetic superexchange interaction is antiferromagnetic for the composition range $0 \leqq x \leqq 0.6$ and ferromagnetic for the compositions $0.7 \leqq x \leqq 1.0$.

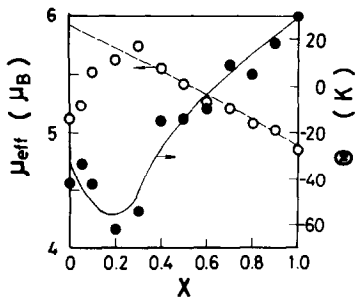

FIG. 4. Effective magnetic moment and paramagnetic Curie temperature vs mole fraction for $Fe(Nb_{1-x}W)O_4$.

(3) Mössbauer Effect

Mössbauer absorption spectra of $Fe(Nb_{0.4}W_{0.6})O_4$ at room temperature and liquid nitrogen temperature are illustrated in Fig. 5. Both spectra consist of two kinds of quadrupole pairs due to the high-spin states of the Fe^{3+} and Fe^{2+} ions. It is clear that the absorption peak around 0 mm/sec^{-1} does

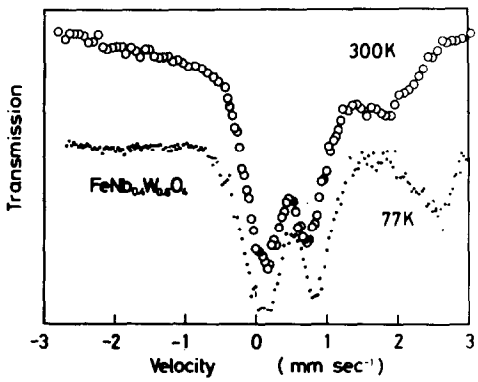

FIG. 5. Mössbauer spectra of $Fe(Nb_{0.4}W_{0.6})O_4$ at room temperature and liquid nitrogen temperature.

not shift with changes in temperature, but the absorption peaks around 1 and 2 mm/sec^{-1} at room temperature shifted to a higher-velocity site at 77°K. The shift of peak in the highest-velocity region is particularly large. These results indicate that the quadrupole splitting due to the Fe^{2+} ions at 77°K is larger than that at 300°K. The values of center shift and quadrupole splitting for Fe^{3+} and Fe^{2+} ions are summarized in Table I.

(4) *Electrical Properties*

The electrical resistivity is illustrated in Fig. 6 as a function of reciprocal temperature in the temperature range 150 to 300°K. It is found that the solid solution system of $Fe(Nb_{1-x}W_x)O_4$ exhibits semiconducting behavior. Log ρ vs $1/T$ is nonlinear below room temperature. The activation energy, E_{act}, obtained from the linear range of the log ρ vs T^{-1} curve is shown as a function of x in Fig. 7. As seen in this figure, the activation energy decreases rapidly from $x = 0$ to $x = 0.2$ and slowly from $x = 0.2$ to $x = 1$, reaching about 0.17 eV.

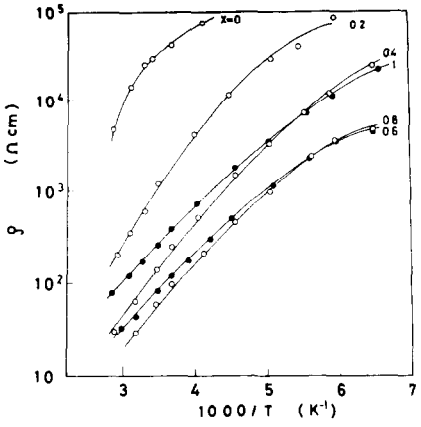

FIG. 6. Electrical resistivity vs reciprocal temperature for $Fe(Nb_{1-x}W_x)O_4$.

Electrical resistivity at constant temperature is shown in Fig. 8 as a function of x. Each ρ–x curve has a minimum value at $x = 0.6$; Table II shows the carrier type in this solid solution system at room temperature determined from the Seebeck effect measurement. It was reported by Larson (*12*) that mixed valency compounds of $Ni_{1-x}Mn_{2+x}O_4$ with spinel-type structure have a

TABLE I

CENTER SHIFT $\delta_{Fe^{n+}}(T)$ AND QUADRUPOLE SPLITTING $\Delta E_{Fe^{n+}}(T)$ FOR $Fe(Nb_{1-x}W_x)O_4$

x	$\delta_{Fe^{3+}}$ (77°K) (mm/sec)	$\delta_{Fe^{3+}}$ (300°K) (mm/sec)	$\Delta E_{Fe^{3+}}$ (77°K) (mm/sec)	$\Delta E_{Fe^{3+}}$ (300°K) (mm/sec)
0	0.48	0.37	0.40	0.37
0.2	0.49	0.39	0.49	0.43
0.4	0.50	0.42	0.57	0.49
0.5	0.50	0.42	0.57	0.49
0.6	0.50	0.46	0.68	0.57
0.8	0.50	0.48	0.72	0.58
x	$\delta_{Fe^{2+}}$ (77°K) (mm/sec)	$\delta_{Fe^{2+}}$ (300°K) (mm/sec)	$\Delta E_{Fe^{2+}}$ (77°K) (mm/sec)	$\Delta E_{Fe^{2+}}$ (300°K) (mm/sec)
0.4	1.16	0.96	2.62	1.62
0.5	1.22	0.96	2.61	1.73
0.6	1.30	0.94	2.43	1.82
0.8	1.34	1.08	2.34	1.62
1.0	1.25	1.10	2.17	1.60

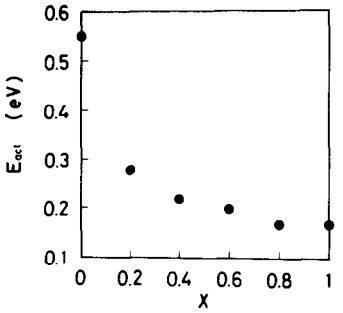

FIG. 7. Activation energy vs mole fracton for $Fe(Nb_{1-x}W_x)O_4$.

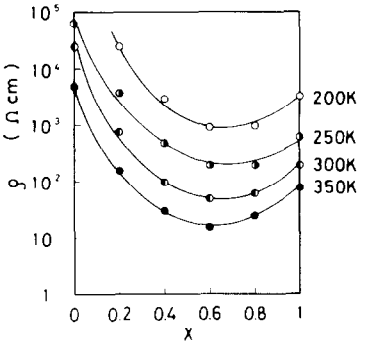

FIG. 8. Electrical resistivity vs mole fraction for $Fe(Nb_{1-x}W_x)O_4$.

minimum value of ρ and a change of carrier type at identical compositions.

The electrical properties of mixed valency compounds have been discussed using a hopping model which assumes hopping of a $3d$ electron from M^n to $M^{(n+1)+}$ induced by lattice vibrations. In order to explain the electrical properties of the solid solution of $Fe(Nb_{1-x}W_x)O_4$ on the basis of a hopping model, this system is divided into three mole fraction regions.

(a) In the mole fraction region near $FeNbO_4$ ($x = 0$), Fe^{3+} ions change their valence state to the divalent state due to the substitution of Nb^{5+} ions by W^{6+} ions to keep electrical neutrality. Fe^{2+} ions located at an octahedral site are surrounded by Fe^{3+} ions through oxygen atoms. The $3d$ electron on the Fe^{2+} ion hops from Fe^{2+} to Fe^{3+}. Therefore, in this case, the carriers are $3d$ electrons and the carrier type is n. The electrical conductivity σ is given by

$$\sigma = ne\mu_e, \tag{1}$$

TABLE II

CARRIER TYPE AT ROOM TEMPERATURE FOR $Fe(Nb_{1-x}W_x)O_4$

x	Carrier type
0	n
0.2	n
0.4	n
0.8	p
1.0	p

where n is the carrier density and μ_e is the mobility of the carrier. Both n and μ_e are functions of x and T, but the dependence of μ_e on x may be weaker than that of n. Figure 8 shows that the electrical conductivity increases with increasing x; this indicates that n increases with increasing x.

(b) In the mole fraction region near $FeWO_4$ ($x = 1.0$), it is assumed that the residual Fe^{3+} ions are in the state of Fe^{2+} ions with a $3d$ hole; the $3d$ hole hops from Fe^{3+} to Fe^{2+}. Therefore, in this case, the carrier is a $3d$ hole and the carrier type is p. σ is given by

$$\sigma = pe\mu_p, \tag{2}$$

where p is the carrier ($3d$ hole) density and μ_p is the mobility of the $3d$ hole. The electrical conductivity decreases with increasing x in this region (Fig. 8) which suggests that p decreases with increasing x.

(c) In the intermediate compositional region, it is assumed that the carriers are $3d$ electrons and holes. Therefore σ is given by

$$\sigma = ne\mu_e + pe\mu_p. \tag{3}$$

In this region, it is assumed that n increases and p decreases with increasing x. The electrical conductivity σ [Eq. (3)] should have a maximum value at the mole fraction corresponding to the boundary between cases (b) and (c), because in general μ_e is larger than μ_p. At this composition the carrier type should change to p type. This is supported by

the electrical behavior of this system in the neighborhood of $x = 0.6$. Therefore $x = 0.6$ is considered the boundary composition.

References

1. R. S. RORTH AND J. L. WARING, *Amer. Mineral.* **49**, 242 (1964).
2. H. CID-DRESDER AND C. ESCOBAR, *Z. Kristallogr.* **127**, 61 (1968).
3. V. D. ÜLKÜ, *Z. Kristallogr.* **124**, 192 (1967).
4. L. G. VAN UITERT, J. J. RUBIN, AND W. A. BONNER, *J. Phys. Chem. Solids* **25**, 1447 (1964).
5. F. A. ROZHDESTVENSKII, G. G. KASIMOV, AND E. J. KRYLOW, *Sov. Phys. Solid State* **11**, 1366 (1969).
6. D. N. ASTROV, N. A. KRYKOVA, R. B. ZORIN, U. A. MAKAROV, R. P. OZEROV, F. A. ROZHDESTVENSKII, V. P. SMIRNOV, A. M. TURCHANINOV, AND N. V. FADEEVA, *Sov. Phys. Crystallogr.* **17**, 1017 (1973).
7. H. A. OBERMAYER, H. DACHS, AND H. SCHRÖCKE, *Solid State Commun.* **12**, 779 (1973).
8. A. W. SLEIGHT AND J. F. WEIHER, *Inorg. Chem.* **7**, 1093 (1968).
9. F. KANAMARU, M. SHIMADA, M. KOIZUMI, AND T. ASAI, *in* "Proceedings, Fourth International Conference on High Pressure, 1974," p. 180.
10. D. ADLER, *Rev. Mod. Phys.* **40**, 714 (1968).
11. L. R. WALKER, G. K. WERTHEIM, AND V. JACCARINO, *Phys. Rev. Lett.***6**, 98 (1961).
12. E. G. LARSON, R. J. ARNOTT, AND D. G. WICKHAM, *J. Phys. Chem. Solids* **23**, 1171 (1962).